**INTERNATIONAL JOURNAL OF OPTIMIZATION IN CIVIL ENGINEERING**
***Int. J. Optim. Civil Eng., 2022; 12(1):69-89***

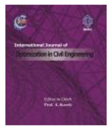

# DAMAGE DETECTION OF TRUSS STRUCTURES VIA GOLD RUSH OPTIMIZATION ALGORITHM

S. Sarjamei, M. Sajjad Massoudi*, † and M. Esfandi Sarafraz
*Department of Civil Engineering, College of Engineering, West Tehran Branch, Islamic Azad University, Tehran, Iran.*

## ABSTRACT

The damage identification of truss constructions was investigated in this work. Damage detection is defined through an inverse optimization problem. A function defined as a combination of mode shapes and natural frequencies is examined to minimize damage structures. This guided approach considerably reduces the computational cost and increases the accuracy of optimization. This index mostly exhibits an acceptable performance. Gold Rush Optimization (GRO), an artificial intelligence system based on the power of human thinking and decision-making, was employed to address damage detection. The programming was done in MATLAB. Validation and verification were carried out using a 10, 25, 200, 272, and 582 bar truss. A comparison between the GRO, MCSS, PSO and TLBO is conducted to show the efficiency of the GRO in finding the global optimum. The results show that utilizing the proposed function and the GRO optimization technique to discover truss damaged structure in the quickest time possible is both reliable and stable.

**Keywords:** structural failure; damage detection; space truss; natural frequencies; mode shapes; gold rush optimization algorithm.

Received: 12 September 2021; Accepted: 20 January 2022

## 1. INTRODUCTION

Earthquakes can harm engineering structures during their usable lives, and the propagation of these damages can result in human and financial losses. It is vital to recognize the damage quickly to avoid such occurrences. Damage detection techniques include both indirect and inverse approaches. The finite element model (FEM) is commonly used to update the system

*Corresponding author: Department of Civil Engineering, College of Engineering, West Tehran Branch, Islamic Azad University, Tehran, Iran.
†E-mail address: massoudi.ms@wtiau.ac.ir (M. Sajjad Massoudi)

model and establish objective functions in the inverse approach. Chou and Ghaboussi [1] used the Genetic Algorithm (GA) to locate structural damage based on residual force and static displacements. A Cooperative Coevolutionary Genetic Algorithm (CCGA) was presented by Boonlong [2] for vibration-based damage detection of cantilever and supported beams. He took into account random noise in the modal features and concluded that the cooperative CCGA outperformed ordinary GA. Natural frequencies and mode shapes are proposed in this study to detect structural damage and prevent such damage [3], [4]. Natural frequencies, mode shapes, and damping are modal parameters of the structure, which are physical properties that include mass, damping, and rigidity [5]. The selected strategy takes the approach of updating the analytical model and treating structural identification as an optimization issue. The discrepancy between the analytical model and the measured (damaged) structure is represented by the defined objective function. The goal is to minimize the objective function or, to put it another way, to converge the analytical model's answers to the responses of the damaged structure. Because of their effectiveness and robustness against uncertainty, meta-heuristic algorithms were used to optimize the objective function. Ettefagh and Akbari [6] developed a method for detecting damage based on FEM updates and Guyan model reduction. Cancelli and Laflamme [7] presented their most recent study on detecting damage using SEREP reduction and particle swarm optimization (PSO). To discover damage locations, Majumdar et al. [8] used Ant Colony Optimization (ACO) to optimize an objective function built using natural frequencies. Their research revealed that the proposed strategy is effective for localization. Damage detection based on MCSS and PSO using modal data was given by Kaveh and Maniat [9]. Only natural frequency changes sensitive to damage were considered by Nobahari and Seyedpoor [10] when they established the objective function. To detect the location and severity of damage to structures, Mehrian et al. [11] proposed two objective functions, one based on the softness matrix and the other based on a mix of natural frequencies and mode shapes. They compared the findings of the particle swarm technique and the charged system search (CSS) particles to solve the damage detection problem. Mishra et al. [12] also evaluated two objective functions, one based on natural frequency changes and the other based on natural frequency and mode shape changes at the same time. They used the ant lion algorithm (ALO). Cha and Buyukozturk [13] proposed a system for detecting the location of various damages utilizing Modal Strain Energy (MSE) as an index and hybrid multi-objective GA as the optimization technique. To demonstrate the resilience of the proposed system, they exploited incomplete mode forms and noise effects. As a two-step strategy for identifying structural deterioration, Kaveh et al. [14] suggested methods that simultaneously analyze changes in natural frequency and mode forms. The rapid water evaporation optimization algorithm was utilized (AWEO). Kim and Lee [15] apply the evolution algorithm to create a new penalty function that improves damage detection and algorithm convergence for the objective function based on vibrational data. By presenting an enhanced version of the evolutionary algorithm and using a penalty function in the objective function based on the soft matrix, Guedria [16] has identified the location and severity of damage in plate structures. Tan et al. [17] combined MSE with Artificial Neural Networks to demonstrate the efficiency of this hybrid technique in detecting single and multiple-damage situations in steel-concrete composite bridges. Kang et al. [18] devised a hybrid Particle Swarm

Optimization (PSO) system that incorporates the Artificial Immune System algorithm. They demonstrated that the proposed approach is reliable and suitable for detecting damage. Other damage detection approaches that use reduction techniques may be found in Kaveh and Dadras [19], Zhu and Huang [20], Ghannadi and Noori [21], Gres and Ulriksen [22], Thambiratnam [23], Öztürk and Baran [24].

In the following, meta-heuristic algorithms have been used to solve damage detection in the optimization problem. Meta-heuristic optimization techniques have become popular in recent decades. One of the most famous optimization algorithms is the Genetic Algorithms (GA). GA was inspired by Charles Darwin's idea of biological evolution. Kaveh and Mahdavi [25], with laws of momentum and energy between collisions bodies, introduced the new algorithm called Colliding Bodies Optimization (CBO). Enhanced Colliding Bodies Optimization (ECBO) introduced by Kaveh and Ilchi Ghazaan [26] improved the function of the CBO algorithm. ECBO uses memory to save some best solutions. Kaveh and Talatahari [27] proposed a meta-heuristic algorithm called the charged system search (CSS). To explore the optimum locations, CSS uses the Coulomb and Gauss laws from physics and Newtonian laws from mechanics to guide the charged particles (CPs). Kaveh and Talatahari [28] used CSS for optimized truss problems. Kaveh and Motie Share [29] improved the function of the CSS algorithm and introduced Magnetic Charged System Search (MCSS). Kaveh and Mirzaei [30] used MCSS for optimized truss problems. Most recently, the Big Bang–Big Crunch algorithm (BB–BC) suggested by Erol [31] and developed by Kaveh, and Talatahari [32] has been proposed. Kaveh and Khayatazad [33] have introduced the Ray Optimization algorithm (RO) with dielectric materials and Snell's refraction law. Gold Rush Optimization (GRO) by Massoudi and Sarjamei [34] has been introduced and used to solve real structural solutions.

This research aimed to optimize damage detection truss structures using the GRO, MCSS, PSO and TLBO algorithms. This study hypothesized that the abilities of the GRO algorithm could reduce the time. The GRO, MCSS, PSO and TLBO algorithms to damage detection truss structures such as 10, 25, 200, 272, and 582 have been investigated.

## 2. MATERIALS AND METHODS

### *2.1 Methodology of damage detection*

The main modal parameters of the structure are derived from Eq (1) in the damage detection method:

$$\left(K-\omega_i^2 M\right)\varphi_i=0 \qquad i=1,2,\dots,n \tag{1}$$

The natural frequency, mode forms in the first mode, stiffness, and mass matrix are represented as $\omega_i$, $\varphi_i$, K, and M, respectively.

Damage is characterized as a loss in stiffness, which is accounted for in the equations by a reduction factor $\beta$. The mass matrix of the structure is thought to be unaffected. The stiffness matrix of an element changes when it is damaged, as seen in Eq (2):

$$[K_{id}] = (1-\beta_i)[K_i] \tag{2}$$

The parameter here ranges from 0 to 1, with 0 denoting no damage and one representing complete damage. The maximum failure rate in this investigation is 0.3, implying a maximum of 30% damage in each element.

Minor damage cannot be diagnosed just based on frequency, according to previous research. When the structure is symmetrical, objective functions based solely on natural frequency variations are insufficient. Because damage to regular and symmetrical structure points results in identical frequency changes, undamaged members can be distinguished as damaged members. Damage of varying intensities and locations, on the other hand, can result in similar alterations in some measured frequencies. Because mode shapes provide more local information than natural frequencies, they are more sensitive to local damage and can be utilized to identify damage directly. The damage detection results are better when the natural frequency and mode shapes are combined in the objective function than utilized independently. The objective function considered for this study is shown in Eq (3):

$$\mathrm{F(X)}=\sqrt{\frac{1}{n}\left(\sum_{i=1}^{n}\left(f_i^a(X)-f_i^c(X)\right)^2+\sum_{i=1}^{n}\sum_{j=1}^{m}\left(\varphi_{ij}^a(X)-\varphi_{ij}^c(X)\right)^2\right)} \tag{3}$$

$X$ is the damage state, and n and m are the numbers of natural frequencies and mode shape in each natural frequency in the objective function, respectively, in Eq (3). The $i^{\text{th}}$ actual (measured) and computed natural frequencies are denoted by $f_i^a$ and $f_i^c$, respectively. $\varphi_{ii}$ is the $i^{\text{th}}$ mode shape's $j^{\text{th}}$ entry. All mode forms are normalized to a unit length before being used in the goal function. The impact on the environment was previously expected to be negligible. In reality, the structure's inherent frequencies do not alter much after the damage-inflicting event, which supports this theory.

As a general conclusion, a penalty function, as indicated in Eq (4), can be considered for the goal function to raise the sensitivity of the target function to the occurrence of damage and uncertainty in the measurement.

$$\begin{aligned}
&Find\ \ X=[\beta_1,\beta_2,\ldots,\beta_{nte}], \quad such\ \ that\ \ 0\le\beta_i\le 1\\
&\text{minimize}\ \ \mathrm{G}(X)=(1+P(X))\times F(X)\\
&P(X)=\frac{ele^d(X)}{nte}
\end{aligned} \tag{4}$$

The unknown damage values for structural elements are shown in Eq (4) by the vector $X$. $P(X)$ is a penalty function applied to the minor objective function $F(X)$ using the multiplication approach. $G(X)$ is the recommended objective function. Assume that the majority of the structural elements are intact and only a few are damaged. As a result, the penalty function is the ratio of the total number of structural elements to the number of damaged elements $ele^d(X)$ from the $X$ solution $(nte)$. Not only is the gap between the modal responses of the actual (measured) and calculated model reduced by applying the penalty function to the objective function, but it also reduces the number of damaged elements and avoids detecting elements that have been wrongly reported as damaged [16].

### *2.2 Gold Rush Optimization (GRO) algorithm*

Damage detection in the optimization issue was solved using the GRO algorithm [34]. Compared to other optimization algorithms, this is a population-based evolutionary algorithm with a fast convergence speed. The Gold Rush Optimization algorithm (GRO) was created using the power of human reasoning and decision-making. The goal is to locate the gold location. A number of people known as operators are stationed in a random location inside the search field to begin. Every stage requires the operators to move together and listen to the sound until they notice an increase in volume, at which point they must halt. Every operator would also listen to the sounds made by other devices and keep an eye out for any equipment that makes a louder sound. The group advances to the location with the loudest sound at each step. Finally, the precise location of the gold is discovered. The flowchart of the GRO algorithm is depicted in Fig. 1.

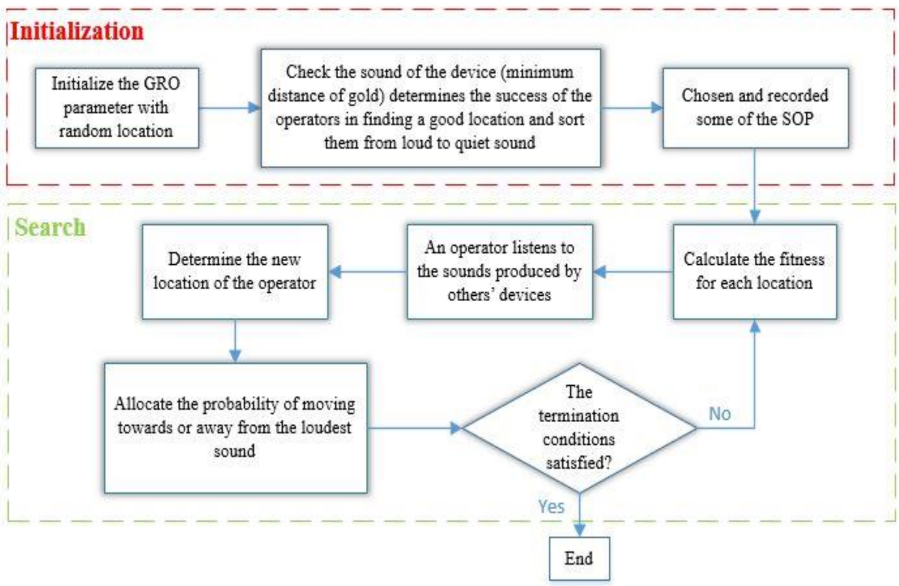


Figure 1. Gold Rush Optimization algorithm

Level 1: Initialization

In Eq (5), each operator is represented at random in one location within the search space. The operators' search spaces are $lb_i$ and $ub_i$. Rand is a random number in the range [0..1].

$$location_i^{(0)} = lb_i + (ub_i - lb_i) * rand \quad , \quad i = 1, 2, \ldots, N \tag{5}$$

Level 2: Monitoring-Choosing the best locations

An operator who is successful in finding the optimal location is called SOP. The top ten percent of operators should be picked and kept in the SOP after each iteration.

Level 3: Fitness-distance

Eq. (6) is used to compute the loudness of each sound (rate), which is the operator with the best chance of finding gold.

$$\text{rate}(i) = \frac{D_i}{\rho_i} * \frac{sound\left(highest\,volume\right) - sound\left(i\right)}{\left(sound\left(highest\,volume\right) - sound\left(lowest\,volume\right) + \varepsilon\right)} \quad (6)$$

The coefficients $\rho_i$, and $D_i$ in Eq. (7) and Eq. (8), respectively, are employed to prevent environmental errors.

$$\rho_i = 2 - \frac{iter}{max_{iter}} \quad (7)$$

$$D_i = \sqrt{\left(x_i - x_j\right)^2 + \left(y_i - y_j\right)^2 + \dots} \quad (8)$$

Each operator will make unique choices based on a mix of sounds in this step. Eq. (9)

$$new\,location(i) = location(i) + md \times \left[\left(rate(j) - rate(i)\right) * \left(location(j) - location(i)\right) * rand\right] \quad (9)$$

The md coefficients denote the move direction as specified by Eq. (10):

$$md = \begin{cases} +1 \Rightarrow towards\ a\ loudest\ sound & \alpha > rand \\ -1 \Rightarrow away\ from\ a\ loudest\ sound & \alpha < rand \end{cases} \quad (10)$$

Level 5: Correct location

Eq. (11) is used to produce new locations if the location obtained in Eq. (9) does not match the problem's criteria. $\beta$ and $\gamma$ coefficients are selected between $0 < \beta < \gamma < 1$.

$$new\,location(i) = \begin{cases} choose\ a\ neighboring\ location & rand < \beta \\ select\ a\ new\ location\ randomly & \beta < rand < \gamma \\ do\,not\,move & \gamma < rand \end{cases} \quad (11)$$

Level 6: Termination

Steps 4 through 6 are performed in a loop until one of the following requirements is met:

1. The maximum number of attempts possible
2. The best location has remained unchanged.
3. The difference between the values of the SOP function and the global optimum is less than a pre-determined predicted threshold.

4. If the difference in objective values between the best and worst locations is less than a particular precision.

The GRO algorithm is applied for Eq. (4) in this study.

The maximum amount of destruction of an element is achieved without the structure falling. MATLAB is used to run the algorithm.

Five numerical examples were analyzed, including a 10, 25, 200, 272, and 582 bar truss to evaluate the efficiency of the suggested method and the optimization algorithm. The results of the GRO, MCSS, PSO and TLBO algorithms damage detection are reviewed.

## 3 NUMERICAL EXAMPLES

In this section, using the structure's natural frequency and the GRO, MCSS, PSO and TLBO algorithms, the structural damage using Eq. (4) is obtained. The technique's effectiveness is shown by five problems such as 10,25, 200, 272, and 582 bar truss were analyzed. For this purpose, damage scenarios, without noise cases, are examined for each problem. All calculations are carried on an Intel corei3 2.3 GHz CPU. The damage results will be more accurate as of the number of modes considered in the structure increases.

A 10-bar truss

The first numerical example is a 10 bar truss problem that has been studied by Kaveh and Zolghadr [3]. The schematic topology and element numbering, as illustrated in Fig. 2. There are six nodes, of which two are fixed. The following are the material properties assumptions for this problem: Material density (ρ)= 2770.0 (kg/$m^3$), Modulus of elasticity (E) = 6.89E10 (N/$m^2$), Added mass 454.0 (kg). The members, which are classified into ten design groups. All of the groups are presented in Fig. 2. Therefore, this problem has ten parameters. The cross-sectional area of each member is taken as 0.0025 ($m^2$).

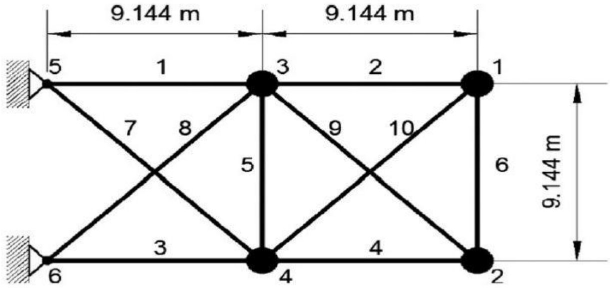


Figure 2. A 10-bar planar truss (Photo reproduced from [3])

The coefficients $\alpha$ = 0.5, $\beta$ = 0.5, and $\gamma$ = 0.75 are considered. Using five operators in each iteration. Two different damage scenarios listed in Table 1 were studied to assess the efficacy of the objective function in recognizing detection.

Table 1: Damage scenarios for 10 bar truss

| Scenarios | Damage elements | Damage severity |
|---|---|---|
| one | 1 | 5% |
| two | 2 | 10% |
| | 4 | 5% |

The 10-bar truss problem is solved ten times. The example uses a maximum number of repeats of 50 as the termination condition.

The optimum results of the GRO algorithm and the actual damages are depicted in Fig. 3 and Table 2. Damage elements are marked in red in the table. Based on the results, the variables of the current research in scenarios one and two are accurate. There is no false detection in all scenarios. The results powerfully demonstrate the capability of the GRO for detecting damages in a 10-bar truss. Also, the TLBOAIS-T and TLBOAIS-S algorithms worked without error in the first scenario and a small error in scenario two. The TLBO algorithm has shown poor performance in both scenarios.

Table 2: Damage detection results of optimization algorithms scenario one and two for the planar 10-bar truss problem

| element | Scenarios One | | | | Scenarios Two | | | |
|---|---|---|---|---|---|---|---|---|
| | GRO | TLBO [35] | TLBOAIS-T[35] | TLBOAIS-S[35] | GRO | TLBO[35] | TLBOAIS-T[35] | TLBOAIS-S[35] |
| 1 | 0.050 | 0.598 | 0.050 | 0.050 | 0.000 | 0.562 | 0.000 | 0.000 |
| 2 | 0.000 | 0.588 | 0.000 | 0.000 | 0.100 | 0.570 | 0.058 | 0.100 |
| 3 | 0.000 | 0.581 | 0.000 | 0.000 | 0.000 | 0.560 | 0.001 | 0.000 |
| 4 | 0.000 | 0.587 | 0.000 | 0.000 | 0.050 | 0.550 | 0.010 | 0.050 |
| 5 | 0.000 | 0.589 | 0.000 | 0.000 | 0.000 | 0.562 | 0.000 | 0.000 |
| 6 | 0.000 | 0.585 | 0.000 | 0.000 | 0.000 | 0.536 | 0.038 | 0.000 |
| 7 | 0.000 | 0.583 | 0.000 | 0.000 | 0.000 | 0.558 | 0.000 | 0.000 |
| 8 | 0.000 | 0.586 | 0.000 | 0.000 | 0.000 | 0.536 | 0.000 | 0.000 |
| 9 | 0.000 | 0.586 | 0.000 | 0.000 | 0.000 | 0.551 | 0.000 | 0.000 |
| 10 | 0.000 | 0.582 | 0.000 | 0.000 | 0.000 | 0.560 | 0.004 | 0.000 |

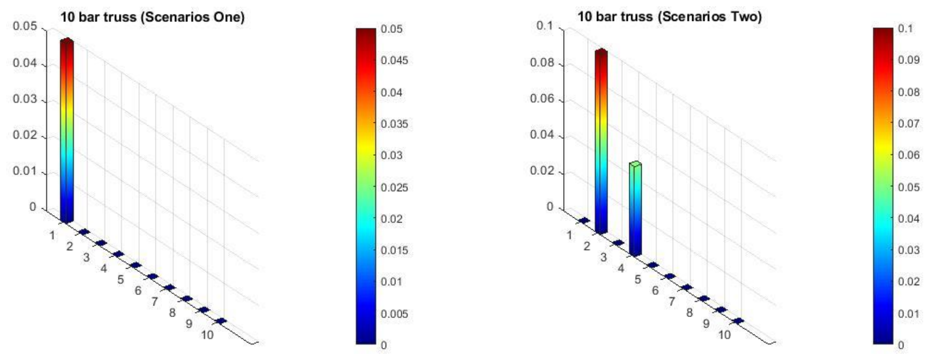


Figure 3. Damage scenarios and GRO evaluation for 10-bar truss

A 25-bar truss

The second numerical example is a 25 bar truss problem that has been studied by Kaveh and Maniat [9]. The schematic topology and element numbering, as illustrated in Fig. 4. There are ten nodes, of which four are fixed. The following are the material properties assumptions for this problem: Material density (ρ)= 0.1 (lbm/in3), Modulus of elasticity (E) = $10^4$ (ksi), L= 25 (in). The members, which are classified into 25 design groups. All of the groups are presented in Fig. 4. Therefore, this problem has 25 parameters. The cross-sectional area of each member is taken as 10 (in$^2$).

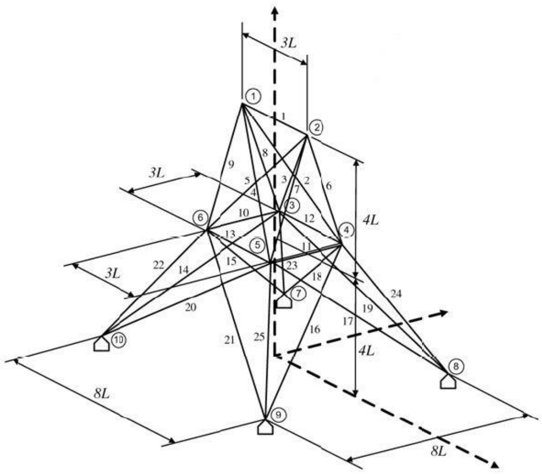

Figure 4. A 25-bar planar truss (Photo reproduced from [9])

The coefficients $\alpha$ = 0.5, $\beta$ = 0.5, and $\gamma$ = 0.75 are considered. Using ten operators in each iteration. Two different damage scenarios listed in Table 3 were studied to assess the efficacy of the objective function in recognizing detection.

Table 3: Damage scenarios for 25-bar truss

| Scenarios | Damage elements | Damage severity |
|---|---|---|
| one | 7 | 15% |
| | 13 | 20% |
| two | 2 | 20% |
| | 10 | 25% |
| | 18 | 15% |

The 25-bar truss problem is solved 15 times. The example uses a maximum number of repeats of 70 as the termination condition.

The optimum results of the GRO algorithm and the actual damages are depicted in Fig. 5 and Table 4. Damage elements are marked in red in the table. Based on the results, the variables of the current research in scenarios one and two are accurate. There is approximately no false detection in all scenarios. The results powerfully demonstrate the capability of the GRO for detecting damages in a 25-bar truss. Also, the PSO algorithm approximately worked without error in the first scenario and a small error in scenario two.

The MCSS algorithm has errors in both scenarios.

Table 4: Damage detection results of optimization algorithms scenario one and two for the planar 25-bar truss problem

| element | Scenarios One | | | Scenarios Two | | |
|---|---|---|---|---|---|---|
| | GRO | MCSS[9] | PSO[9] | GRO | MCSS[9] | PSO[9] |
| 1 | 0.0 | 0.089 | 0.0 | 0.0 | 0.0 | 0.11 |
| 2 | 0.0 | 0.0 | 0.0 | 0.20 | 0.195 | 0.20 |
| 3 | 0.0 | 0.0 | 0.0 | 0.0 | 0.0 | 0.0 |
| 4 | 0.0 | 0.0 | 0.0 | 0.0 | 0.0 | 0.0 |
| 5 | 0.0 | 0.0 | 0.0 | 0.0 | 0.0 | 0.0 |
| 6 | 0.0 | 0.0 | 0.0 | 0.0 | 0.0 | 0.0 |
| 7 | 0.15 | 0.145 | 0.146 | 0.0 | 0.0 | 0.0 |
| 8 | 0.0 | 0.0 | 0.0 | 0.0 | 0.0 | 0.0 |
| 9 | 0.0 | 0.0 | 0.0 | 0.0 | 0.0 | 0.0 |
| 10 | 0.0 | 0.094 | 0.0 | 0.25 | 0.252 | 0.27 |
| 11 | 0.0 | 0.0 | 0.0 | 0.0 | 0.025 | 0.021 |
| 12 | 0.0 | 0.0 | 0.0 | 0.0 | 0.049 | 0.0 |
| 13 | 0.0 | 0.0 | 0.0 | 0.045 | 0.0 | 0.213 |
| 14 | 0.012 | 0.0 | 0.0 | 0.0 | 0.0 | 0.04 |
| 15 | 0.0 | 0.0 | 0.0 | 0.0 | 0.0 | 0.0 |
| 16 | 0.0 | 0.0 | 0.0 | 0.0 | 0.0 | 0.0 |
| 17 | 0.0 | 0.0 | 0.0 | 0.0 | 0.0 | 0.0 |
| 18 | 0.0 | 0.0 | 0.0 | 0.15 | 0.147 | 0.148 |
| 19 | 0.0 | 0.0 | 0.0 | 0.0 | 0.0 | 0.0 |
| 20 | 0.0 | 0.0 | 0.0 | 0.0 | 0.0 | 0.0 |
| 21 | 0.0 | 0.0 | 0.0 | 0.0 | 0.0 | 0.0 |
| 22 | 0.0 | 0.0 | 0.0 | 0.0 | 0.0 | 0.0 |
| 23 | 0.20 | 0.204 | 0.204 | 0.0 | 0.0 | 0.0 |
| 24 | 0.0 | 0.0 | 0.0 | 0.0 | 0.0 | 0.0 |
| 25 | 0.0 | 0.0 | 0.0 | 0.0 | 0.0 | 0.0 |

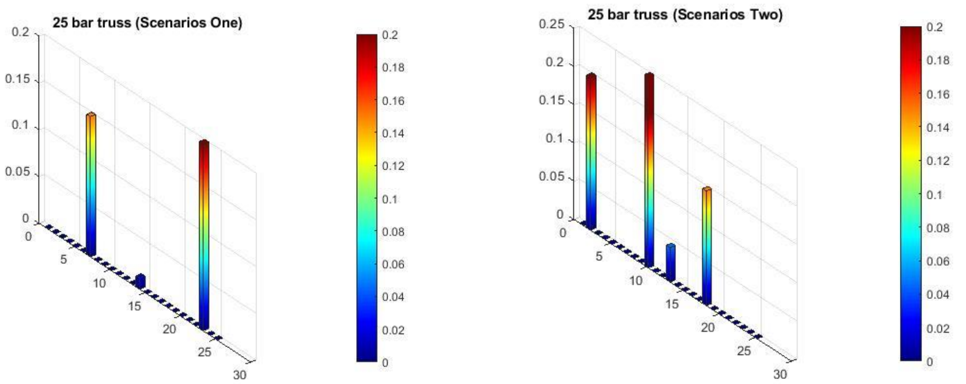


Figure 5. Damage scenarios and GRO evaluation for 25-bar truss

A 200-bar planar truss structure

The first numerical example is a 200 bar truss design problem that has been studied by Kaveh and Zaerreza [36]. The schematic topology and element numbering, as illustrated in Fig. 6. There are 77 nodes, of which two are fixed. The members are all made of steel. The following are the material properties assumptions for this problem: Material density (ρ)= 0.283 ($lb/in^2$), Modulus of elasticity (E) = 30,000 (ksi). The members, which are classified into 29 design groups. All of the groups are presented in Ref [36]. Therefore, this problem has 29 parameters. The cross-sectional area of each member is taken as 2 ($in^2$).

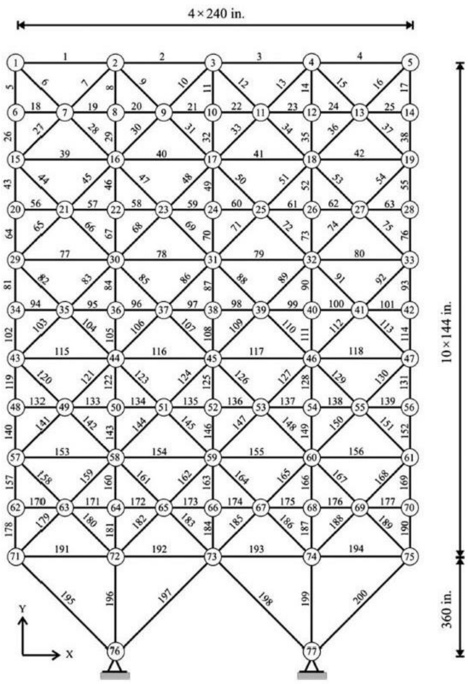


Figure 6. 200-bar spatial truss (Photo reproduced from[36])

The coefficients $\alpha$ = 0.5, $\beta$ = 0.5, and $\gamma$ = 0.85 are considered. Using 30 operators in each iteration. Three different damage scenarios listed in Table 5 were studied to assess the efficacy of the objective function in recognizing detection.

Table 5: Damage scenarios for 200-bar spatial truss

| Scenarios | Damage elements | Damage severity |
|---|---|---|
| one | 10 | 15% |
| | 20 | 15% |
| two | 5 | 20% |
| | 15 | 20% |
| | 25 | 20% |
| three | 3 | 10% |
| | 17 | 10% |
| | 27 | 10% |

The 200-bar truss problem is solved 20 times. The example uses a maximum number of repeats of 300 as the termination condition.

The optimum results of the GRO algorithm and the actual damages are depicted in Fig. 7 and Table 6. Damage elements are marked in red in the table. Based on the results, the variables of the current research in scenarios one and two are closer to reality. There is approximately no false detection in scenario three. The results powerfully demonstrate the capability of the GRO for detecting damages in a 200-bar truss.

Table 6: Damage detection results of optimization algorithms scenario one, two, and three for the planar 200-bar tower truss problem

| Element | Scenarios One | Scenarios Two | Scenarios Three |
|---|---|---|---|
| | GRO | GRO | GRO |
| 1 | 0.0 | 2.4231682E-4 | 0.0 |
| 2 | 0.0 | 0.0 | 0.0095649399 |
| 3 | 0.0 | 0.0 | 0.10 |
| 4 | 0.0014729438 | 0.0 | 0.0 |
| 5 | 0.0 | 0.20 | 0.0042135879 |
| 6 | 0.0 | 0.000029861 | 0.0 |
| 7 | 0.0419345824 | 0.0 | 0.0 |
| 8 | 0.0 | 0.0 | 0.0 |
| 9 | 0.0132751164 | 0.031360889 | 0.0000083305 |
| 10 | 0.15 | 0.0 | 0.0037165482 |
| 11 | 0.0175424938 | 0.0 | 0.0 |
| 12 | 0.0 | 0.0 | 0.0 |
| 13 | 0.0000041215 | 0.0 | 0.0145680913 |
| 14 | 0.0004932854 | 0.002187752 | 0.0 |
| 15 | 0.0058358293 | 0.20 | 4.7253433E-4 |
| 16 | 0.0275114934 | 0.004241669 | 0.0054239287 |
| 17 | 0.0075963115 | 0.024769076 | 0.10 |
| 18 | 0.0195527417 | 0.0 | 0.0064621552 |
| 19 | 0.0 | 0.0 | 0.0 |
| 20 | 0.15 | 0.0275212723 | 0.0005499315 |
| 21 | 0.0 | 0.0 | 0.0 |
| 22 | 0.0 | 0.0 | 0.0024152415 |
| 23 | 0.0085412276 | 0.0000375215 | 0.0 |
| 24 | 0.0 | 0.0241583769 | 0.0 |
| 25 | 0.0158850457 | 0.20 | 7.0456227E-5 |
| 26 | 0.0 | 0.0 | 0.0052452456 |
| 27 | 0.0212457789 | 0.0 | 0.10 |
| 28 | 0.0 | 0.0028452279 | 0.0 |
| 29 | 0.0 | 0.0 | 0.0 |

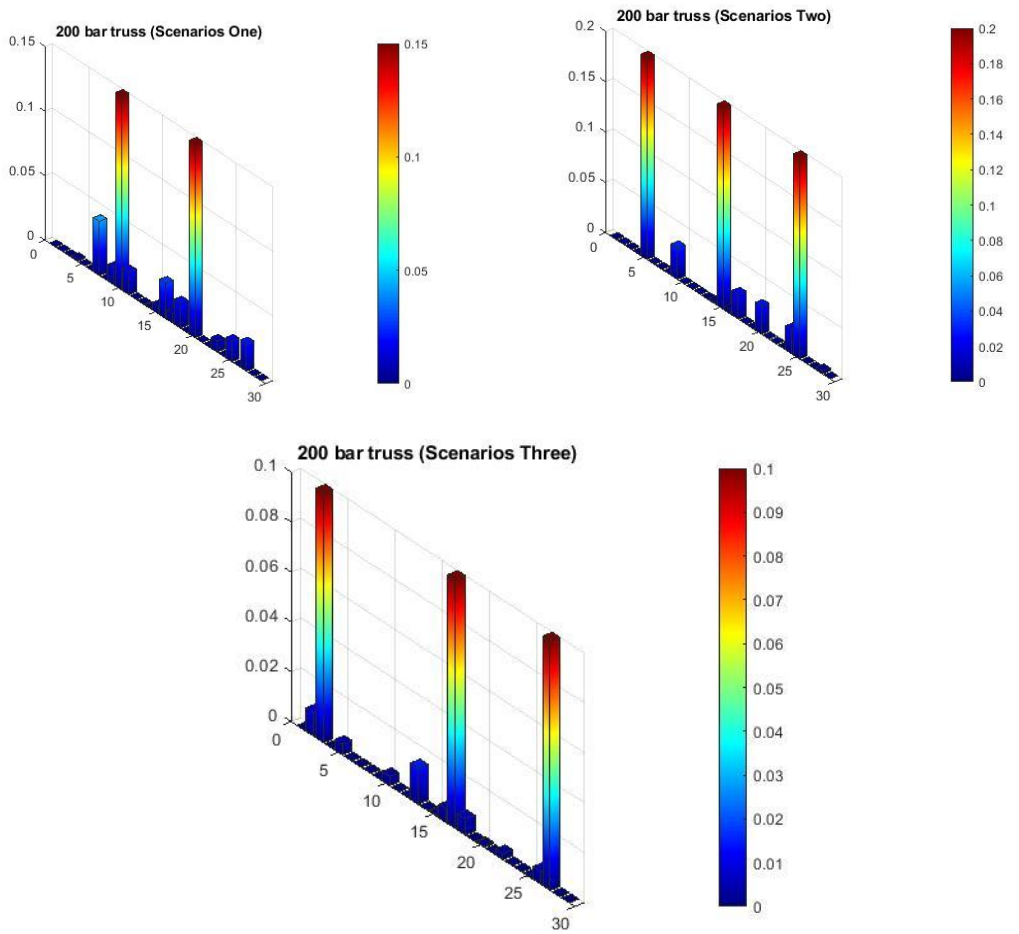


Figure 7. Damage scenarios and GRO evaluation for 200-bar spatial truss

A 272-bar transmission truss structure

The second numerical example is a 272-bar planer truss that has been studied by Kaveh and Massoudi [37]. The schematic topology and element numbering, as illustrated in Fig. 8. There are 65 nodes, of which four are fixed. The members are all made of steel. The following are the material properties assumptions for this problem: Modulus of elasticity E = 2e8 (KN/m2). The members, which are classified into 28 design groups. All of the groups are presented in Ref [37]. Therefore, this problem has 28 parameters. The cross-sectional area of each member is taken as 2 ($in^2$).

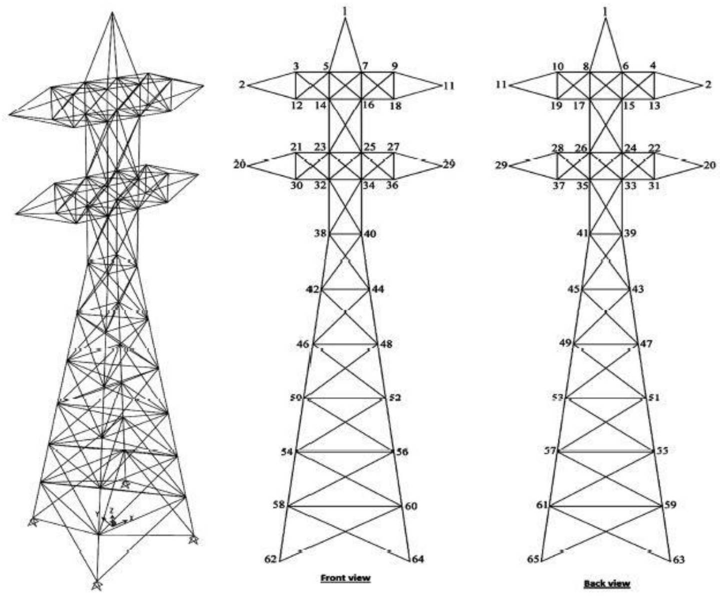


Figure 8. 272-bar spatial truss in design problem(Photo reproduced from[37])

The coefficients $\alpha$ = 0.5, $\beta$ = 0.5, and $\gamma$ = 0.85 are considered. Using 35 operators in each iteration. Three different damage scenarios listed in Table 7 were studied to assess the efficacy of the objective function in recognizing detection.

Table 7: Damage scenarios for 272-bar planer truss

| Scenarios | Damage elements | Damage severity |
|---|---|---|
| one | 10 | 15% |
| | 20 | 15% |
| two | 5 | 20% |
| | 15 | 20% |
| | 25 | 20% |
| three | 3 | 10% |
| | 13 | 10% |
| | 23 | 10% |

The 272-bar planer truss is solved 20 times. The example uses a maximum number of repeats of 350 as the termination condition.

The optimum results of the GRO algorithm and the actual damages are depicted in Fig. 9 and Table 8. Damage elements are marked in red in the table. Based on the results, the variables of the current research in all scenarios are closer to reality. Few elements were mistakenly identified as damaged parts. The results powerfully demonstrate the capability of the GRO for detecting damages in 272-bar transmission truss.

Table 8: Damage detection results of optimization algorithms scenario one, two, and three for the 272-bar transmission truss structure

| Element | Scenarios One GRO | Scenarios Two GRO | Scenarios Three GRO |
|---|---|---|---|
| 1 | 0.0042452452 | 0.0 | 0.0043292824 |
| 2 | 0.0 | 0.0 | 0.0 |
| 3 | 0.0 | 0.005643551 | 0.10 |
| 4 | 0.0026883107 | 0.004345315 | 0.0 |
| 5 | 0.0 | 0.20 | 0.0 |
| 6 | 0.0065431613 | 0.0 | 0.0004245825 |
| 7 | 0.0 | 0.0 | 0.0007102824 |
| 8 | 0.0 | 0.068135131 | 0.0 |
| 9 | 0.0589315125 | 0.0 | 0.0344071905 |
| 10 | 0.15 | 0.0 | 0.0053646865 |
| 11 | 0.0257541743 | 0.0651351615 | 0.0 |
| 12 | 0.0 | 0.0 | 0.0324164782 |
| 13 | 0.15 | 0.00 | 0.10 |
| 14 | 0.0006918156 | 0.0019754515 | 0.0 |
| 15 | 0.0 | 0.20 | 0.0000071642 |
| 16 | 0.0152527471 | 0.0064524556 | 0.0090549283 |
| 17 | 0.0014534231 | 0.0 | 0.0 |
| 18 | 0.0485157255 | 0.0 | 0.0 |
| 19 | 0.0 | 0.0043532465 | 7.8418067E-7 |
| 20 | 0.15 | 0.0322126135 | 0.0021552315 |
| 21 | 0.0 | 0.0 | 0.0012670822 |
| 22 | 0.0 | 0.0 | 0.0012156326 |
| 23 | 0.0065134453 | 0.0 | 0.10 |
| 24 | 0.0 | 0.0146397829 | 0.0 |
| 25 | 0.0 | 0.20 | 1.6561614E-2 |
| 26 | 0.0 | 0.0 | 0.0084531654 |
| 27 | 0.0186453115 | 0.0000374356 | 0.0 |
| 28 | 0.0 | 0.0003546144 | 0.0 |

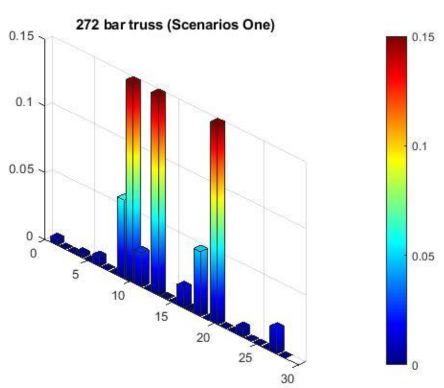


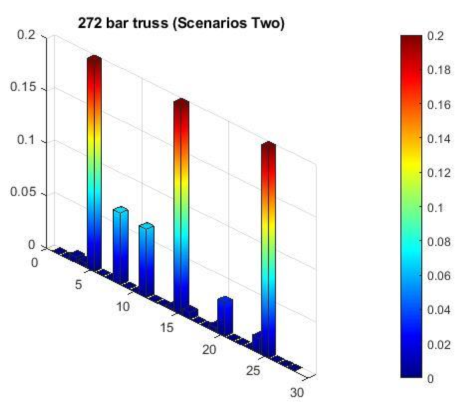

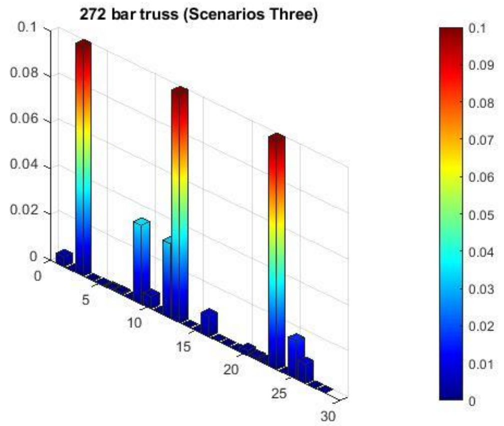


Figure 9. Damage scenarios and GRO evaluation for 272-bar planer truss

A 582-bar spatial skeletal tower

The third numerical example is a 582-bar spatial skeletal tower that has been studied by Sonmez [38]. The schematic topology and element numbering, as illustrated in Fig. 10. There are 153 nodes, of which ten are fixed. The following are the material properties assumptions for this problem: Material density ρ= 0.28 lb/in$^3$ (7.833 t/m$^3$), Modulus of elasticity (E) = 29,000 ksi (200 GPa). The members, which are classified into 32 design groups. All of the groups are presented in Fig. 6. Therefore, this problem has 32 parameters. The cross-sectional area of each member is taken as 3 (in$^2$).

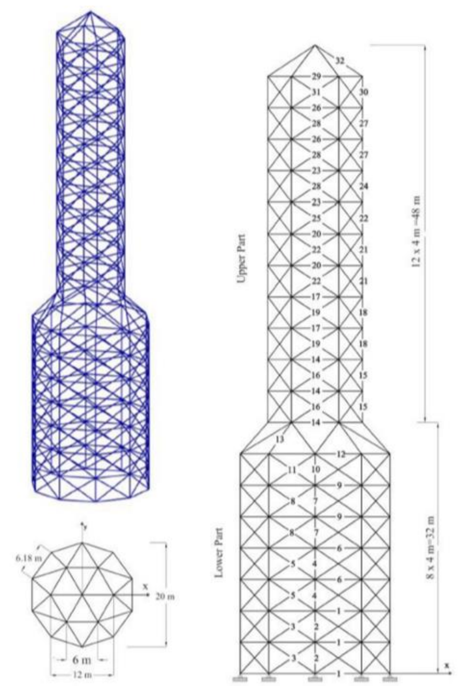


Figure 10. 582-bar spatial skeletal tower design problem (Photo reproduced from [38])

The coefficients $\alpha$ = 0.5, $\beta$ = 0.5, and $\gamma$ = 0.85 are considered. Using 40 operators in each iteration. Three different damage scenarios listed in Table 9 were studied to assess the efficacy of the objective function in recognizing detection.

Table 9: Damage scenarios for 582-bar spatial skeletal tower

| Scenarios | Damage elements | Damage severity |
|---|---|---|
| one | 13 | 20% |
| | 23 | 20% |
| two | 5 | 15% |
| | 15 | 15% |
| | 25 | 15% |
| three | 10 | 10% |
| | 20 | 10% |
| | 30 | 10% |

The 582-bar planer truss is solved 20 times. A total of 70 operators are on the job. The example uses a maximum number of repeats of 350 as the termination condition.

The optimum results of the GRO algorithm and the actual damages are depicted in Fig. 11 and Table 10. Damage elements are marked in red in the table. Based on the results, the variables of the current research in scenarios one and two are closer to reality. There is approximately no false detection in scenario three. The results powerfully demonstrate the capability of the GRO for detecting damages in the 582-bar skeletal tower.

Table 10: Damage detection results of optimization algorithms scenario one, two, and three for the 582-bar skeletal tower

| Element | Scenarios One | Scenarios Two | Scenarios Three |
|---|---|---|---|
| | GRO | GRO | GRO |
| 1 | 0.0 | 0.002163161 | 0.0021231123 |
| 2 | 0.0 | 0.0 | 0.0003115316 |
| 3 | 0.0 | 0.0 | 0.0 |
| 4 | 0.0034316431 | 0.004316115 | 0.0 |
| 5 | 0.0 | 0.15 | 0.0006471253 |
| 6 | 0.0033264516 | 0.0 | 0.0 |
| 7 | 0.0 | 0.0 | 0.0003216153 |
| 8 | 0.0 | 0.021316139 | 0.0124031238 |
| 9 | 0.0 | 0.032136892 | 0.0 |
| 10 | 0.0021513543 | 0.0 | 0.10 |
| 11 | 0.0134941723 | 0.0 | 0.0051521965 |
| 12 | 0.0 | 0.0 | 0.0 |
| 13 | 0.20 | 1.516418E-4 | 0.0 |
| 14 | 0.0003216116 | 0.006843511 | 0.0 |
| 15 | 0.0 | 0.15 | 0.0000034645 |
| 16 | 0.0651656875 | 0.007161669 | 0.0010420083 |
| 17 | 0.0016412875 | 8.0334194E-3 | 0.0 |

| | | | |
|---|---|---|---|
| 18 | 0.0115641985 | 0.0 | 0.0 |
| 19 | 0.0 | 0.0 | 0.0436511635 |
| 20 | 3.0334194E-4 | 0.0246341351 | 0.10 |
| 21 | 0.0 | 6.0645656E-2 | 0.0 |
| 22 | 0.0 | 0.0 | 0.0 |
| 23 | 0.20 | 0.0 | 0.0004234164 |
| 24 | 0.0109768912 | 0.0343161351 | 0.0 |
| 25 | 7.5645184E-2 | 0.15 | 0.0 |
| 26 | 0.0 | 0.0354651267 | 0.0041316515 |
| 27 | 0.0 | 0.0 | 0.0 |
| 28 | 0.0065464137 | 0.0015465594 | 0.0 |
| 29 | 0.0 | 0.0 | 0.0054131615 |
| 30 | 0.0 | 0.0 | 0.10 |
| 31 | 0.0021959987 | 5.0541544E-8 | 0.0046812595 |
| 32 | 0.0079096455 | 0.0025225652 | 0.0 |

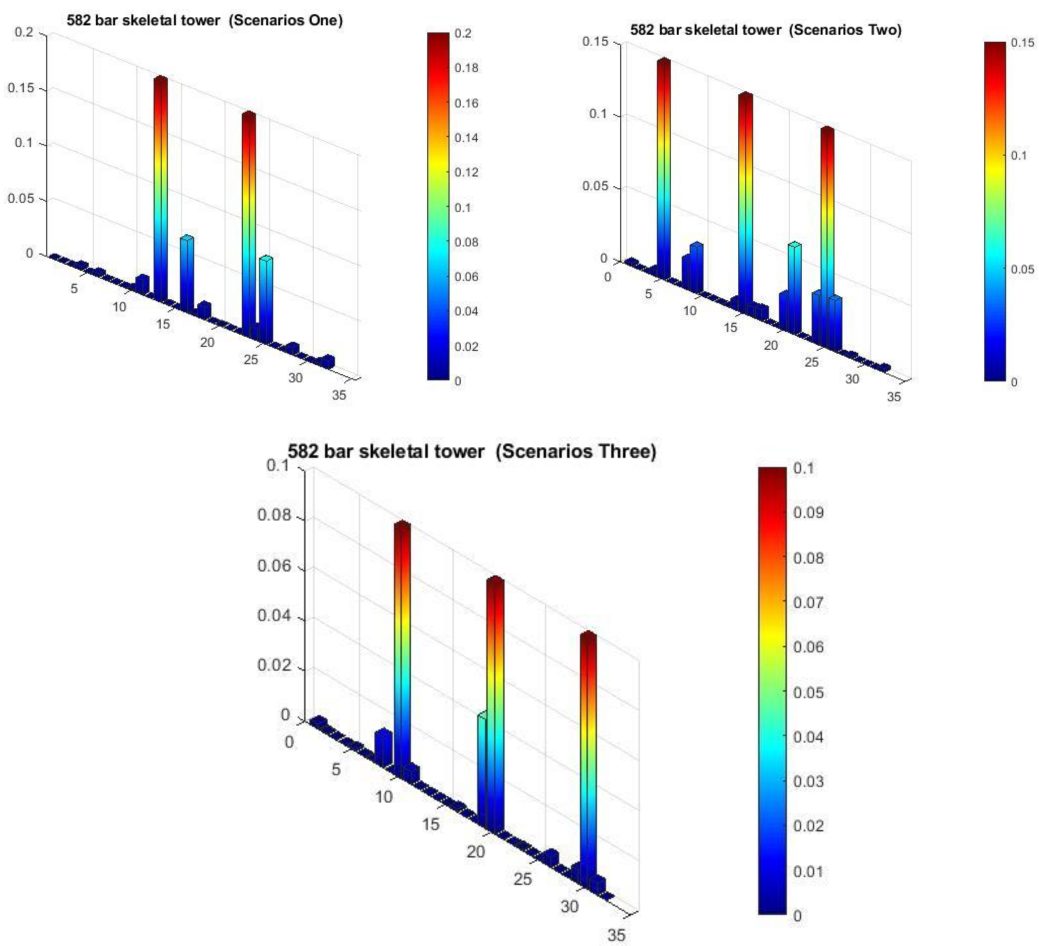


Figure 11. Damage scenarios and GRO evaluation for 582-bar skeletal tower

## CONCLUSION

The damage detection of truss structures using natural frequency changes is considered an inverse optimization issue in this paper. Natural frequencies are calculated using the GRO, TLBO, and MCSS meta-heuristic optimization algorithm's outputs. The Gold Rush Optimization method created by Massoudi and Sarjamei was used to identify as many global optimal solutions as possible. The ability of the GRO, MCSS, PSO and TLBO algorithms has been tested by modeling 10, 25, 200, 272, and 582 bar trusses. For 10, 25, 200, 272, and 582 bar trusses, the results confirm that the GRO can effectively perform damage localization so that all faulty elements are considered optimization variables. Therefore, the GRO not only reduces the computational cost of inverse damage detection but also increases accuracy. The recommended future research should compare the findings of various meta-heuristic optimization methods to those of GRO.

## REFERENCES


1. Chou JH, Ghaboussi J. Genetic algorithm in structural damage detection, *Comput. Struct* 2001; **79**(14): 1335-53. doi: 10.1016/S0045-7949(01)00027-X.
2. Boonlong K. Vibration-based damage detection in beams by cooperative coevolutionary genetic algorithm, *Adv Mech Eng* 2014; **6**: 624949. doi: 10.1155/2014/624949.
3. Kaveh A, Zolghadr A. An improved CSS for damage detection of truss structures using changes in natural frequencies and mode shapes, *Adv Eng Softw.*2015; **80**(C): 93–100. doi: 10.1016/J.ADVENGSOFT.2014.09.010.
4. Kaveh A. *Applications of Metaheuristic Optimization Algorithms in Civil Engineering*, 2017.
5. Fan W, Qiao P. Vibration-based damage identification methods: A review and comparative study, *Struct Heal Monit* 2011; **10**(1): 83–111. doi: 10.1177/1475921710365419.
6. Ettefagh MM, Akbari H, Asadi K, Abbasi F. New structural damage-identification method using modal updating and model reduction, *Archive Proceedings Of The Institution Of Mechanical Engineers Part C Journal Of Mechanical Engineering Science* 2014; 229(6): 1041–1059. doi: 10.1177/0954406214542966.
7. Cancelli A, Laflamme S, Alipour A, Sritharan S, Ubertini F. Vibration-based damage localization and quantification in a pre-tensioned concrete girder using stochastic subspace identification and particle swarm model updating, *Struct Heal Monit* 2019; **19**(2): 587–605. doi: 10.1177/1475921718820015.
8. Majumdar A, Maiti DK, Maity D. Damage assessment of truss structures from changes in natural frequencies using ant colony optimization, *Appl. Math Comput* 2012; **218**(19): 9759-72. doi: https://doi.org/10.1016/j.amc.2012.03.031.
9. Kaveh A, Maniat M. Damage detection based on MCSS and PSO using modal data, *Smart Struct Syst* 2015; **15**(5): 1253-70.
10. Nobahari M, Seyedpoor SM. Structural damage detection using an efficient correlation-

based index and a modified genetic algorithm, *Math. Comput Model* 2011; **53**(9–10): 1798–1809. doi: 10.1016/J.MCM.2010.12.058.

11. Mehrian SZ, Amrei SAR, Maniat M, Nowruzpour SM. Structural health monitoring using optimizing algorithms based on flexibility matrix approach and combination of natural frequencies and mode shapes, *Int J Struct Eng* 2016; **7**(4): 398. doi: 10.1504/IJSTRUCTE.2016.079287.
12. Mishra M, Barman SK, Maity D, Maiti DK. Ant lion optimization algorithm for structural damage detection using vibration data, *J Civil Struct Heal Monit* 2018; **9**(1): 117-36. doi: 10.1007/S13349-018-0318-Z.
13. Cha YJ, Büyüköztürk O. Structural damage detection using modal strain energy and hybrid multiobjective optimization, *Comput Aided Civil Infrastruct Eng* 2015; **30**: 347-58.
14. Kaveh A, Hosseini Vaez SR, Hosseini P, Fathali MA. A new two-phase method for damage detection in skeletal structures, *Iran J Sci Technol Trans Civil Eng* 2018; 43(1): 49-65. doi: 10.1007/S40996-018-0190-4.
15. Kim NIl, Kim S, Lee J. Vibration-based damage detection of planar and space trusses using differential evolution algorithm, *Appl Acoust* 2019; **148**: 308-21. doi: 10.1016/J.APACOUST.2018.08.032.
16. Ben Guedria N. An accelerated differential evolution algorithm with new operators for multi-damage detection in plate-like structures, *Appl Math Model* 2020; **80**: 366-83. doi: 10.1016/J.APM.2019.11.023.
17. Tan ZX, Thambiratnam DP, Chan THT, Gordan M, Abdul Razak H. Damage detection in steel-concrete composite bridge using vibration characteristics and artificial neural network, *Struct Infrastruct Eng* 2020; **16**(9): 1247-61. doi: 10.1080/15732479.2019.1696378.
18. Kang F, Li J, Xu Q. Damage detection based on improved particle swarm optimization using vibration data, *Appl Soft Comput* 2012; **12**(8): 2329-35. doi: https://doi.org/10.1016/j.asoc.2012.03.050.
19. Kaveh A, Dadras A. Structural damage identification using an enhanced thermal exchange optimization algorithm, *Eng Optim* 2018; **50**(3): 430-51. doi: 10.1080/0305215X.2017.1318872.
20. Zhu JJ, Huang M, Lu ZR. Bird mating optimizer for structural damage detection using a hybrid objective function, *Swarm Evol Comput* 2017; **35**: 41–52. doi: 10.1016/J.SWEVO.2017.02.006.
21. Ghannadi P, Kourehli SS, Noori M, Altabey WA. Efficiency of grey wolf optimization algorithm for damage detection of skeletal structures via expanded mode shapes, *Adv Struct Eng* 2020; **23**(13): 2850-65. doi: 10.1177/1369433220921000.
22. Gres S. Dalgaard Ulriksen Ma, Döhler M, Johansen RJ, Andersen P, Damkilde L, Andreas Nielsen S. Statistical methods for damage detection applied to civil structures, *Procedia Eng* 2017; 199: 1919-24. doi: 10.1016/J.PROENG.2017.09.280.
23. Randiligama SMCM, Thambiratnam D, Chan THT. Damage detection in hyperbolic cooling towers using vibration based, *in Advances in Engineering Materials, Structures and Systems: Innovations, Mechanics and Applications*, 1st Editio, London, 2019: pp. 2005-2010.
24. Öztürk A, Baran E, Tort C. Nonlinear Fiber modeling of steel-concrete partially

composite beams with channel connectors, *KSCE J Civil Eng* 2019; **23**: 2227-42. doi: 10.1007/s12205-019-1163-2.
25. Kaveh A, Mahdavi VR. Colliding bodies optimization method for optimum discrete design of truss structures, *Comput Struct* 2014; **70**(1): 1–12. doi: 10.1016/j.compstruc.2014.04.006.
26. Kaveh A, Ilchi Ghazaan M. Enhanced colliding bodies optimization for design problems with continuous and discrete variables, *Adv Eng Softw* 2014; **77**: 66–75. doi: http://dx.doi.org/10.1016/j.advengsoft.2014.08.003.
27. Kaveh A, Talatahari S. A novel heuristic optimization method: charged system search, *Acta Mech* 2010; **3**(10). doi: 10.1007/s12192-010-0223-9.
28. Kaveh A, Talatahari S. Optimal design of skeletal structures via the charged system search algorithm, *Struct Multidisc Optim* 2010; 41(6): 893–911, , doi: 10.1007/s00158-009-0462-5.
29. Kaveh A, Motie Share MA, Moslehi M. Magnetic charged system search: A new meta-heuristic algorithm for optimization, *Acta Mech* 2013; **224**(1): 85–107. doi: 10.1007/s00707-012-0745-6.
30. Kaveh A, Mirzaei B, Jafarvand A. An improved magnetic charged system search for optimization of truss structures with continuous and discrete variables, *Appl Soft Comput J* 2015; **28**: 400-10. doi: 10.1016/j.asoc.2014.11.056.
31. Erol OK, Eksin I. A new optimization method: Big Bang–Big Crunch, *Adv Eng Softw* 2006; **37**(2): 106-11. doi: 10.1016/j.advengsoft.2005.04.005.
32. Kaveh A, Talatahari S. Size optimization of space trusses using Big Bang–Big Crunch algorithm, *Comput Struct* 2009; **87**(17–18): 1129-40. doi: 10.1016/j.compstruc.2009.04.011.
33. Kaveh A, Khayatazad M. A new meta-heuristic method: Ray Optimization, *Comput Struct* 2012; **112–113**(10): 283-94. doi: 10.1016/j.compstruc.2012.09.003.
34. Sarjamei S, Massoudi MS, Esfandi Sarafraz M. Gold Rush Optimization Algorithm, *Iran Univ Sci Technol* 2021; **11**(2): 291-327, Accessed: Jul. 04, 2021. [Online]. Available: http://ijoce.iust.ac.ir/article-1-476-en.html.
35. Shahrouzi M, Sabzi AH. Damage detection of truss structures by hybrid immune system and teaching–learning-based optimization, *Asian J Civil Eng* 2018; **19**(7): 811-25. doi: 10.1007/s42107-018-0065-9.
36. Kaveh A, Zaerreza A. Shuffled shepherd optimization method a new Meta-heuristic algorithm, *Eng Comput* 2020; **37**(7). doi: 10.1108/EC-10-2019-0481.
37. Kaveh A, Massoudi MS. Multi -objective optimization of structures using Charged System Search, *Sci Iran* 2014; 21(6): 1845-60.
38. Sonmez M. Performance comparison of metaheuristic algorithms for the optimal design of space trusses, *Arab J Sci Eng* 2018; 43(10): 5265-81. doi: 10.1007/s13369-018-3080-y.